

Domain-wall trapping in a ferromagnetic nanowire network

E. Saitoh,^{a)} M. Tanaka, and H. Miyajima

Department of Physics, Keio University, Yokohama 223-8522, Japan

T. Yamaoka

Seiko Instruments Inc., Matsudo 270-2222, Japan

(Presented on 13 November 2002)

The magnetic domain configuration in a submicron $\text{Ni}_{81}\text{Fe}_{19}$ wire network has been investigated by magnetic force microscopy. To improve the responsivity of the magnetic force microscope, an active quality factor autocontrol method was adopted. In the remanent state, domain walls were observed trapped firmly at the vertexes of the network. The magnetic domain configurations appear to minimize the exchange energy at the vertexes. These results indicate that the magnetic property of the ferromagnetic network can be described in terms of the uniform magnetic moments of the wires and interwire magnetic interactions at the vertexes. The observed structure of the domain walls is well reproduced by micromagnetic simulations. © 2003 American Institute of Physics.

[DOI: 10.1063/1.1544499]

I. INTRODUCTION

Magnetics in submicron ferromagnetic wires has attracted great interest in recent years.¹⁻⁴ In magnetic wires of smaller diameter than the typical extension of the domain wall, the magnetization is restricted to being directed either parallel or antiparallel to the wire axis due to magnetic shape anisotropy. This makes it possible to investigate magnetics in single-domain ferromagnets in a controllable manner. The magnetization process in submicron ferromagnetic wires has been studied in detail.¹⁻³ Until now, however, few studies have focused on interaction among the ferromagnetic wires. This article discusses the magnetic domain configuration in a ferromagnetic wire-based network structure. Results of experiments indicate that the remanent states of the ferromagnetic network are well described in terms of the interwire magnetic interactions at the vertexes.

II. EXPERIMENT

The sample investigated in the present study is a two-dimensional network comprising $\text{Ni}_{81}\text{Fe}_{19}$ wire-based honeycomb structure, which was fabricated by the lift-off technique using electron beam lithography. First, thin polymethyl methacrylate resist (ZEP-520) of 100 nm in thickness was spin coated onto thermally oxidized Si substrate. The resist mask was then patterned with an electron beam at 20 keV in beam energy. After the development, $\text{Ni}_{81}\text{Fe}_{19}$ was deposited by electron-beam evaporation in a vacuum of 1×10^{-8} Torr at 0.5 nm/s deposition rate. The sample was obtained after the resist mask was removed in a solvent (2-butanon). An atomic force microscope (AFM) image of the sample is shown in Fig. 1. The size of the sample is as follows: the width of the wire $w = 55$ nm, the length of the wire $l = 400$ nm, and the thickness is $t = 20$ nm. Magnetic domain structures of the sample were observed by magnetic force

microscopy (MFM) together with AFM. A scanning microscope system (SPI3800N/SPA300HV, SII) equipped with an evacuated (10^{-6} Torr) sample chamber was used in dynamic force mode. The tip of the probe covered with CoPtCr thin film was magnetized before each observation. The distance between probe and sample for MFM measurement was set as 10–20 nm. To improve the responsivity of the MFM, the quality factor of the cantilever was optimized to be around 3000. This is achieved via implementation of an electric feedback loop in the cantilever's driver,^{5,6} which controls the effective quality factor of the cantilever automatically. The method allows investigation of domain wall structures in detail.

III. RESULTS AND DISCUSSION

Figure 2 exemplifies a MFM image and corresponding schematic domain configuration for remanent state after the

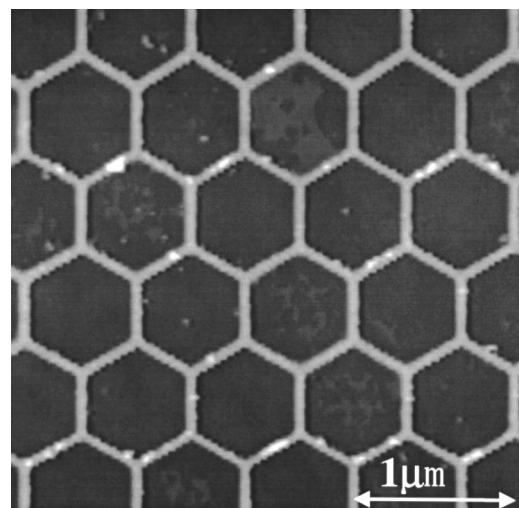


FIG. 1. AFM image for the sample. The size of the wire sample is as follows: wire width $w = 55$ nm, wire length $l = 400$ nm, and wire thickness $t = 20$ nm.

^{a)}Electronic mail: eizi@phys.keio.ac.jp

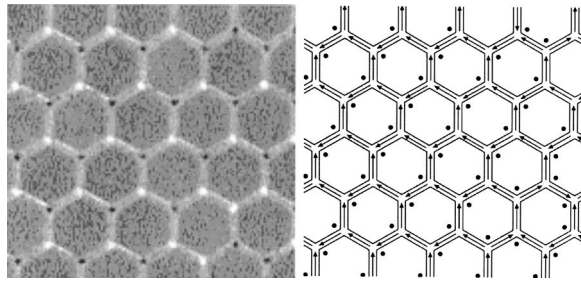


FIG. 2. MFM image and corresponding schematic magnetic domain configuration for the remanent state of the $\text{Ni}_{81}\text{Fe}_{19}$ honeycomb network. The initial magnetic field (1 kOe) was perpendicular to the network. Closed circles in the right panel represent leakage fields due to domain walls.

application of an external magnetic field (1 kOe) perpendicular to the film plane. Clear leakage field signals due to the divergence of the magnetization was observed at each vertex, signaling domain walls at vertexes.⁷ Notably, no domain wall features were observed in the wire parts in the present network. This indicates that the vertex traps the domain wall firmly and allows the wire part to be single domain. The result suggests that the magnetic property of the ferromagnetic network can be described in terms of the uniform magnetic moments of each wire and interactions among the wires at the vertexes.

The magnetic domain configurations appear to minimize the exchange energy at the vertexes. The observed direction of magnetization \mathbf{M}_i in each wire (i) was found to be so determined that the vector sum of \mathbf{M}_i for three wires jointed at each vertex N , $\sum_{i \in N} \mathbf{M}_i$, must not be zero vector. This is the so-called “two-in, one-out” or “one-in, two-out” magnetic structure around a vertex. Such a rule excluding “three-in” or “three-out” magnetic structures ($\sum_{i \in N} \mathbf{M}_i = 0$) can be accounted for by the large magnetic energy loss due to the abrupt magnetization rotation at the vertex in the structures, indicating that the magnetic energy at the vertex dominates the magnetic properties in the network. In spite of such a strong rule at the vertexes, each wire part remains single domain. This signals that the single domain of each wire is significantly stable.

The above observation allows the magnetic properties in the present network to be modeled in terms of the following effective energy formula:

$$E(\{\mathbf{M}_i\}) = -J \sum_N \left| \sum_{i \in N} \mathbf{M}_i \right|^2 - \sum_i \mathbf{H} \cdot \mathbf{M}_i. \quad (1)$$

Here, $J/4|\mathbf{M}_i|^2$ and \mathbf{H} are the energy difference between $\sum_{i \in N} \mathbf{M}_i \neq 0$ configuration and $\sum_{i \in N} \mathbf{M}_i = 0$ configuration, and external magnetic field, respectively. The \sum_N denotes the sum over all the vertexes. The second term in Eq. (1) represents the total Zeeman energy. Note that \mathbf{M}_i is restricted to direct parallel or antiparallel to the each wire axis. Expanding Eq. (1) gives the following simple formula comprising nearest-neighbor interaction and Zeeman term:

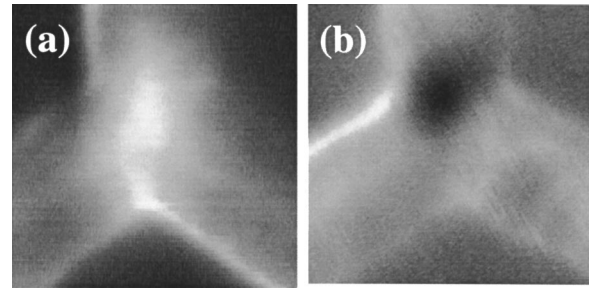


FIG. 3. Magnification of two typical MFM images around vertex parts in remanent state of the $\text{Ni}_{81}\text{Fe}_{19}$ honeycomb network. The initial magnetic field (1 kOe) was applied perpendicular to the network.

$$E(\{\mathbf{M}_i\}) = -2J \sum_{\langle i,j \rangle} \mathbf{M}_i \cdot \mathbf{M}_j - \sum_i \mathbf{H} \cdot \mathbf{M}_i + \text{const}. \quad (2)$$

The $\sum_{\langle i,j \rangle}$ denotes the sum all over the nearest-neighbor pairs of wire parts. The formula shows an analogy between the present wire-based network and the Heisenberg-spin model with strong uniaxial magnetic anisotropy, and provides a guideline for designing magnetic properties in ferromagnetic wire-based networks.

Finally, let us briefly discuss the magnetic structure of the domain walls. Figure 3 shows magnified MFM images around vertexes to present the structure of the domain wall in detail. We found two types of domain wall configuration, which are shown in Figs. 3(a) and 3(b), respectively. In one type described in Fig. 3(a), the domain wall is trapped at a corner of the vertex and extends toward the center of the opposite wire. In the other type described in Fig. 3(b), the domain wall is localized at a boundary between a wire and the junction. Such a feature of the domain wall can be described in terms of micromagnetic calculation. Figure 4 shows two magnetic configurations around the vertex for the remanent state obtained from a micromagnetic simulation using the OOMMF program,⁸ which integrates the Landau–Lifshitz equation on a two-dimensional grid (5 nm×5 nm). The directions of the initial magnetic field (10 Oe) in each calculation are indicated by arrows in Fig. 4. The calculation well reproduces the two domain wall structures obtained by MFM and demonstrates that the structure critically depends on the direction of the small initial magnetic field. These results suggest that the two distinct domain structures at the vertexes can be accounted for by a spatially distributed in-

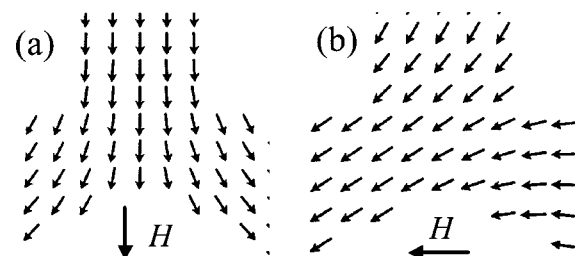


FIG. 4. Magnetic configuration for the vertex part of the $\text{Ni}_{81}\text{Fe}_{19}$ honeycomb network obtained from a micromagnetic simulation based on the Landau–Lifshitz equation. Arrows indicate the directions of the small (10 Oe) initial magnetic field.

plane component, or deviation from perpendicular direction, of the internal magnetic field generated by the network itself, which may arise in the course of the demagnetization.

IV. SUMMARY

In summary, the magnetic domain configuration in a two-dimensional $\text{Ni}_{81}\text{Fe}_{19}$ network comprising a wire-based submicron honeycomb structure was observed using magnetic force microscope. Magnetic domain walls are trapped firmly at the vertexes of the network. The results indicate that the interwire magnetic interaction at the vertexes governs the magnetic properties of ferromagnetic wire-based network.

ACKNOWLEDGMENT

This work was supported by a Grant-in-Aid from the Ministry of Education, Science and Culture of Japan.

- ¹K. Hong and N. Giordano, *J. Magn. Magn. Mater.* **151**, 396 (1995).
- ²Y. Otani *et al.*, *IEEE Trans. Magn.* **34**, 1096 (1998).
- ³U. Ruediger *et al.*, *Appl. Phys. Lett.* **73**, 1298 (1998).
- ⁴T. Ono *et al.*, *J. Appl. Phys.* **85**, 6181 (1999).
- ⁵T. Yamaoka, K. Watanabe, Y. Shirakawabe, and K. Chinone, *J. Magn. Soc. Jpn.* (in press).
- ⁶A. D. L. Humphris, A. N. Round, and M. J. Miles, *Surf. Sci.* **491**, 468 (2001).
- ⁷A. Hirohata *et al.*, *J. Magn. Magn. Mater.* **226–230**, 1485 (2001).
- ⁸M. J. Donahue and D. G. Porter, <http://math.nist.gov/oommf/>.